ASIAN JOURNAL OF CIVIL ENGINEERING (BUILDING AND HOUSING) VOL. 13, NO. 4 (2012)
PAGES 531-555

RISK REDUCTION AND EXTERNALLY FRP RETROFITTING OF RC COLUMNS SUBJECTED TO EXTREME LOADING CONDITIONS

A.R. Mortezaei*[a] and S.M. Zahrai[b]
[a]Department of Civil Engineering, Engineering Faculty, Semnan Branch, Islamic Azad University, Semnan, Iran.
[b]Center of Excellence for Engineering and Management of Infrastructures, School of Civil Engineering, University of Tehran, Tehran, Iran

Received: 29 August 2011; **Accepted**: 28 December 2011

ABSTRACT

Iran is a country of particular geopolitical significance owing to its location in the Middle East and central Eurasia. Owing to its strategic location, Iran has been the centre of attention for traders, businessmen and big powers for a long time. Therefore, it might be exposed at risk. The recognition necessity of risk and the resisting trend is essential for structural engineering. The analysis and design of reinforced concrete structures subjected to extreme loading condition such as blast loads require a detailed understanding of blast phenomena and the dynamic response of various structural elements. In this paper, the response of RC columns subjected to constant axial loads and lateral blast loads is examined. Different shapes of columns, i.e. square, rectangular and circular shape, are considered in this research. A nonlinear finite element program is used to model RC columns with different boundary conditions and using the mesh less method to reduce mesh distortions. For the response calculations, a constant axial force is first applied to the column and then, lateral blast load is applied and the response time history is calculated. Blast load effects on the columns quantified in terms of failure mechanisms through simulation of the whole column detailing in the nonlinear finite element program. According to the analysis results, a retrofitting scheme using FRP wraps is designed and validated with a blast load test. Comparison of results clearly demonstrates that columns with externally FRP retrofitting can withstand higher levels of blast loads. It means that retrofitting RC columns with FRP is a proficient way to ensure protection of buildings under the blast loading.

Keywords: Extreme load conditions; blast; retrofitting; FRP; nonlinear finite element.

* E-mail address of the corresponding author: a.mortezaei@semnaniau.ac.ir (A.R. Mortezaei)

1. INTRODUCTION

A bomb explosion within or immediately nearby a building can cause terrible damage on the building's external and internal structural frames, collapsing of walls, blowing out of large expanses of windows, and shutting down of critical systems. Loss of life and injuries to occupants can result from many causes, including direct blast-effects, structural collapse, debris impact, fire, and smoke. The indirect effects can combine to inhibit or prevent timely evacuation, thereby contributing to additional casualties. In this way, passive defense can be used. Passive defense means, measures taken to reduce the probability of and to minimize the effects of damage caused by aggressive action without the intention of taking the initiative. Due to the threat from such extreme loading conditions, efforts have been made during the past three decades to develop methods of structural analysis and design to resist blast loads. Studies were conducted on the behavior of structural concrete subjected to blast loads. These studies gradually enhanced the understanding of the role that structural details play in affecting the behavior. Figure 1 shows the damages to a building under the blast load.

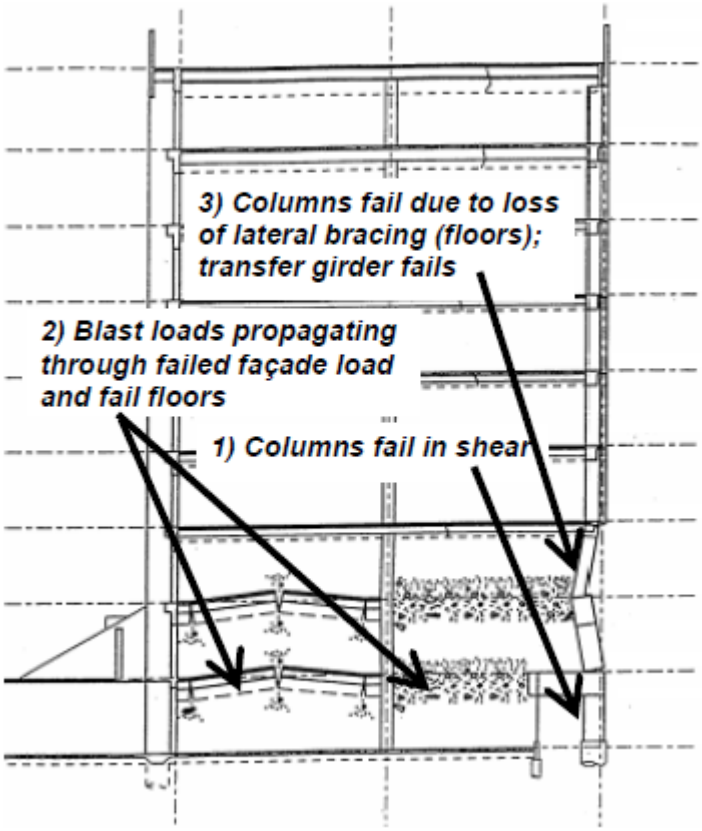

Figure 1. Damages to a building under the blast load

Blast loads are applied over a significantly shorter period of time than seismic loads. Thus, material strain rate effects become critical and must be accounted for in predicting connection performance for short duration loadings such as blast. Also, blast loads generally

will be applied to a structure nonuniformly, i.e., there will be a variation of load amplitude across the face of the building, and severely reduced blast loads on the sides and rear of the building away from the blast. Figure 2 shows a general comparison between an acceleration record from the 2003 Bam earthquake [1] and a blast load time history. It is apparent that the 14-second-long ground shaking from the Bam earthquake lasted approximately 1500 times longer than the 9 ms initial blast pulse. The effects of blast loads are generally local, leading to locally severe damage or failure. Vice-versa, seismic loads are ground motions applied uniformly across the base or foundation of a structure. All components in the structure are subjected to the shaking associated with this motion.

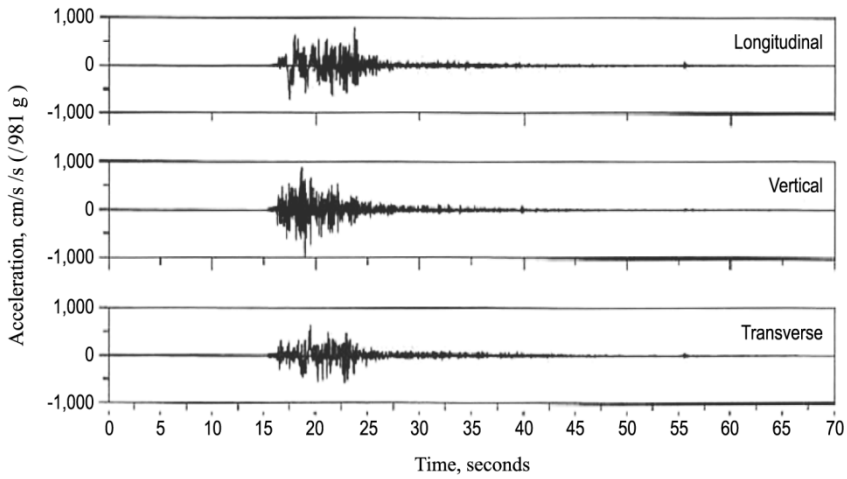

(a)

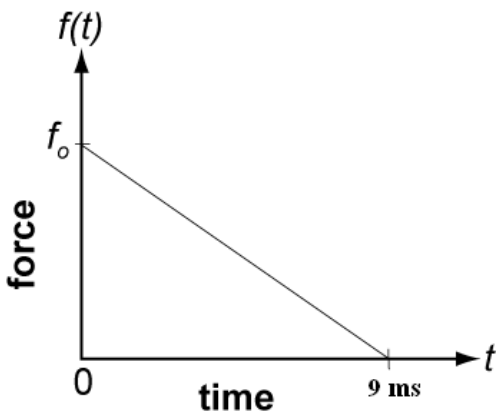

(b)

Figure 2. Comparison between (a) an acceleration record from the 2003 Bam earthquake and (b) a blast load time history

In the past few decades considerable emphasis has been given to problems of blast and earthquake. The earthquake problem is rather old, but most of the knowledge on this subject has been accumulated during the past sixty years. The blast problem is rather new. Due to

different accidental or intentional events, the behavior of structural components subjected to blast loading has been the subject of considerable research effort in recent years. Conventional structures, particularly that above grade, normally are not designed to resist blast loads; and because the magnitudes of design loads are significantly lower than those produced by most explosions, conventional structures are susceptible to damage from explosions. With this in mind, developers, architects and engineers increasingly are seeking solutions for potential blast situations, to protect building occupants and the structures.

Disasters have demonstrated the need for a thorough examination of the behavior of columns subjected to blast loads. To provide adequate protection against explosions, the design and construction of public buildings are receiving renewed attention of structural engineers. Difficulties that arise with the complexity of the problem, which involves time dependent finite deformations, high strain rates, and nonlinear inelastic material behavior, have motivated various assumptions and approximations to simplify the models. These models span the full range of complexity from single degree of freedom systems to general purpose finite element programs such as ABAQUS, ANSYS, and so on. The methods available for prediction of blast effects on buildings structures are empirical, semi-empirical and numerical methods [2].

Empirical methods are essentially correlations with experimental data. Most of these approaches are limited by the extent of the underlying experimental database. The accuracy of all empirical equations diminishes as the explosive event becomes increasingly near field. Semi-empirical methods are based on simplified models of physical phenomena. The attempt is to model the underlying important physical processes in a simplified way. These methods are dependent on extensive data and case study. The predictive accuracy is generally better than that provided by the empirical methods. Numerical methods are based on mathematical equations that describe the basic laws of physics governing a problem. These principles include conservation of mass, momentum, and energy. In addition, the physical behavior of materials is described by constitutive relationships.

2. PAST STUDIES

Luccioni *et al*. [3] presented the analysis of the structural failure of a reinforced concrete building caused by a blast load. The results showed that collapse was due to a gravitational mechanism originated by the destruction of the lower columns. In this case, the explosive charge was determined based on other data, but the demolition of the front block of the building analyzed produced with a smaller charge.

Shi *et al*. [4] proposed a new method for progressive collapse analysis of reinforced concrete frame structures by considering nonzero initial conditions and initial damage to adjacent structural members under blast loading. In their research, a three-storey two-span RC frame was used as an example to demonstrate the proposed method. Numerical results were compared with those obtained using the alternative load path method and was found that the proposed method with a minor and straightforward extension of the simplified procedure is efficient and reliable in simulating the progressive collapse process of RC frame structures.

Khadid *et al*. [5] studied the fully fixed stiffened plates under the effect of blast loads to

determine the dynamic response of the plates with different stiffener configurations and considered the effect of mesh density, time duration and strain rate sensitivity. They used the finite element method and the central difference method for the time integration of the nonlinear equations of motion to obtain numerical solutions.

Pandey *et al*. [6] studied the effects of an external explosion on the outer reinforced concrete shell of a typical nuclear containment structure. The analysis has been made using appropriate nonlinear material models till the ultimate stages. An analytical procedure for nonlinear analysis by adopting the above model has been implemented into a finite element code DYNAIB.

Remennikov [7] studied the methods for predicting bomb blast effects on buildings. Simplified analytical techniques used for obtaining conservative estimates of the blast effects on buildings. Numerical techniques including Lagrangian, Eulerian and finite element modelling used for accurate prediction of blast loads on commercial and public buildings.

Marchand and Alfawakhiri [8] reviewed the contents of American Institute of Steel Construction for facts give a general science of blast effects with the help of numbers of case studies of the building which were damaged due to the blast loading. They also studied the dynamic response of a steel structure to the blast loading and showed the behavior of ductile steel column and steel connections for the blast loads.

Dharaneepathy *et al*. [9] studied the effects of the stand-off distance on tall shells of different heights, carried out with a view to study the effect of distance (ground-zero distance) of charge on the blast response.

Shope [10] studied the response of wide flange steel columns subjected to constant axial load and lateral blast load. The finite element program ABAQUS was used to model with different slenderness ratio and boundary conditions. Non-uniform blast loads were considered. Changes in displacement time histories and plastic hinge formations resulting from varying the axial load were examined.

Borvik *et al*. [11] studied the response of a steel container as closed structure under the blast loads. They used the mesh less methods based on the Lagrangian formulations to reduce mesh distortions and numerical advection errors to describe the propagation of blast load. A methodology was proposed for the creation of inflow properties in uncoupled and fully coupled Eulerian–Lagrangian LS-DYNA simulations of blast loaded structures.

Ngo *et al*. [12] for their study on blast loading and blast effects on structures, gave an overview on the analysis and design of structures subjected to blast loads phenomenon for understanding the blast loads and dynamic response of various structural elements.

Starossek [13] have studied progressive collapse of bridges. He proposed an approach for designing against progressive collapse and presented a set of corresponding design criteria, including requirements, design objectives, design strategies, and verification procedures. In addition to the better-known design methods providing specific local resistance or alternate load paths, an approach based on isolation by compartmentalization was presented. He observed that the terms continuity, redundancy, and robustness should be carefully distinguished when considering progressive collapse of bridges.

Bazant and Verdure [14] investigated the mechanics of progressive collapse. Rather than using classical homogenization, they found it more effective to characterize the continuum by an energetically equivalent snap-through.

3. RESEARCH SIGNIFICANCE

The analysis and design of structures subjected to blast loads require a detailed understanding of blast phenomena and the dynamic response of various structural elements. This gives a comprehensive overview of the effects of explosion on structures. In this paper, the response of RC columns with and without FRP strengthening subjected to constant axial loads and lateral blast loads is examined and performance of different components of column during blast events, identify typical mechanisms responsible for causing failure of typical components are investigated. Different shapes of columns, i.e. square, rectangular and circular shape, are considered in this research. A nonlinear finite element program is used to model RC columns with different boundary conditions and using the mesh less method to reduce mesh distortions. For the response calculations, a constant axial force is first applied to the column and then, lateral blast load is applied and the response time history is calculated.

4. CHARACTERISTICS OF BLAST PHENOMENON

In general, an explosion is the result of a very rapid release of large amounts of energy within a limited time. The time duration for blast is typically in the range of 5 to 10 ms with loadings in the range of several thousands of Newton per square meters. Explosions can be categorized on the basis of their nature as physical and chemical events.

The sudden release of energy initiates a pressure wave in the surrounding medium, known as a shock wave as shown in Figure 3. When an explosion takes place, the expansion of the hot gases produces a pressure wave in the surrounding air. As this wave moves away from the centre of explosion, the inner part moves through the region that was previously compressed and is now heated by the leading part of the wave. As the pressure waves moves with the velocity of sound, the temperature is about 3000°-4000°C and the pressure is nearly 300 kilobar of the air causing this velocity to increase. The inner part of the wave starts to move faster and gradually overtakes the leading part of the waves. After a short period of time the pressure wave front becomes abrupt, thus forming a shock front. The maximum overpressure occurs at the shock front and is called the peak overpressure. Behind the shock front, the overpressure drops very rapidly to about one-half the peak overpressure and remains almost uniform in the central region of the explosion. An expansion proceeds, the overpressure in the shock front decreases steadily; the pressure behind the front does not remain constant, but instead, fall off in a regular manner. After a short time, at a certain distance from the centre of explosion, the pressure behind the shock front becomes smaller than that of the surrounding atmosphere and so called negative-phase or suction.

The front of the blast waves weakens as it progresses outward, and its velocity drops towards the velocity of the sound in the undisturbed atmosphere. This sequence of events is shown in Figure 3, the overpressure at time t1, t2…..t6 are indicated. In the curves marked t1 to t5, the pressure in the blast has not fallen below that of the atmosphere. In the curve t6 at some distance behind the shock front, the overpressure becomes negative. This is better illustrated in Figure 4. Throughout the pressure-time profile, two main phases can be observed; portion above ambient is called positive phase of duration (t_d), while that below

ambient is called negative phase of duration (t_d). The negative phase is of a longer duration and a lower intensity than the positive duration. As the stand-off distance increases, the duration of the positive-phase blast wave increases resulting in a lower-amplitude, longer-duration shock pulse.

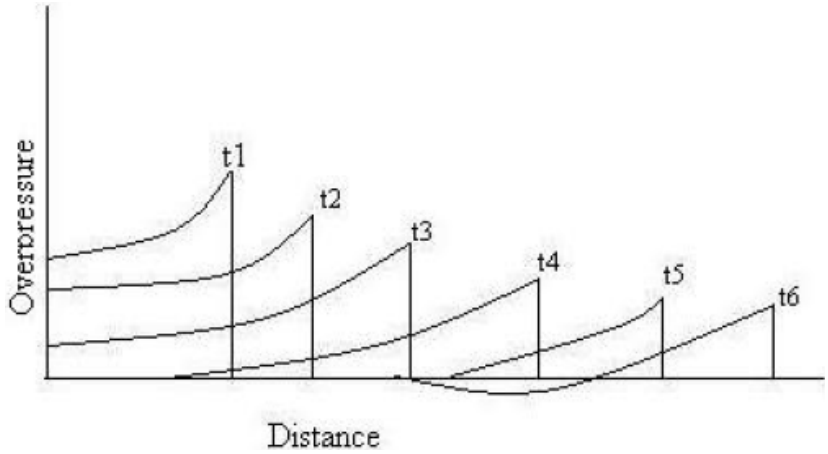

Figure 3. Variation of overpressure with distance from centre of explosion at various times

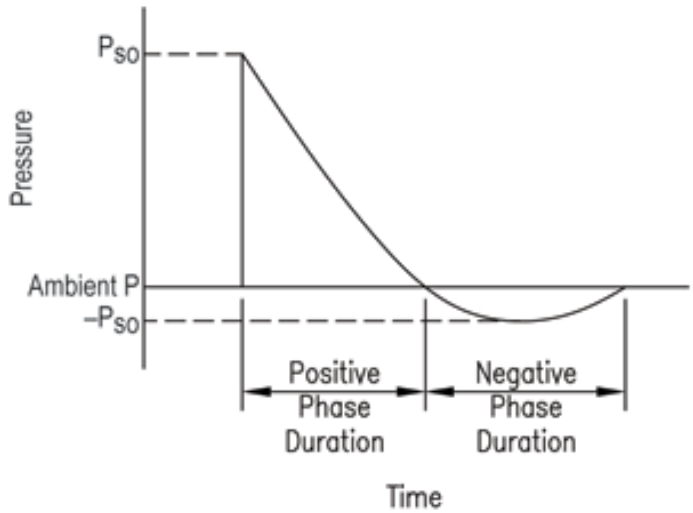

Figure 4. The variation of overpressure with distance at a given time from centre of explosion

Charges situated extremely close to a target structure impose a highly impulsive, high intensity pressure load over a localized region of the structure; charges situated further away produce a lower-intensity, longer-duration uniform pressure distribution over the entire structure (Figure 5). Eventually, the entire structure is engulfed in the shock wave, with reflection and diffraction effects creating focusing and shadow zones in a complex pattern around the structure. During the negative phase, the weakened structure may be subjected to impact by debris that may cause additional damage.

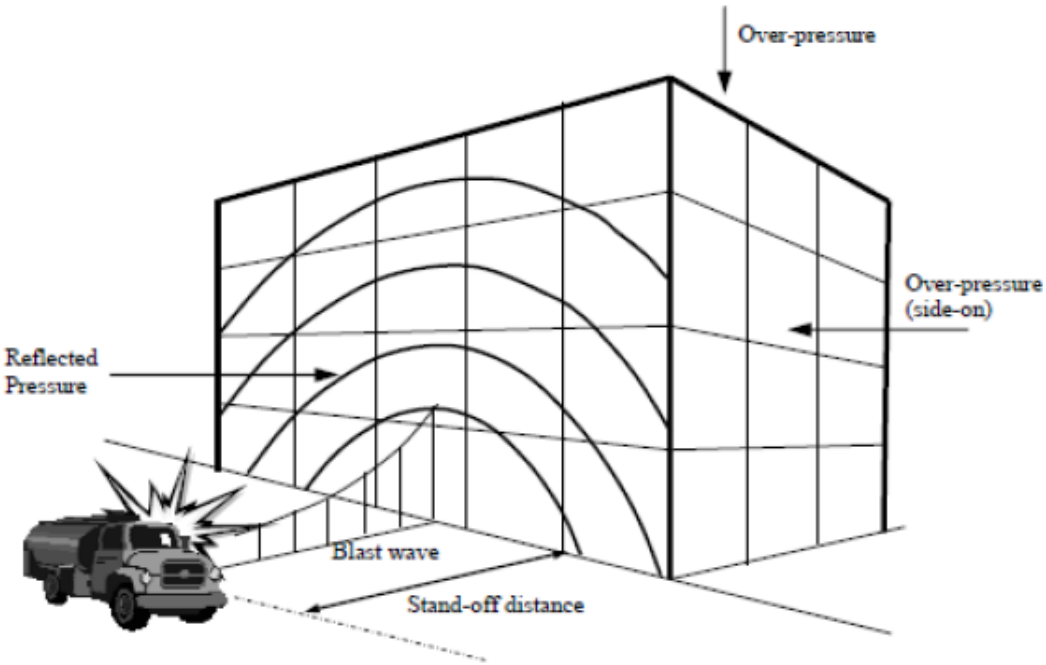

Figure 5. Blast loads on a building

If the exterior building walls are capable of resisting the blast load, the shock front penetrates through window and door openings, subjecting the floors, ceilings, walls, contents, and people to sudden pressures and fragments from shattered windows, doors, etc. Building components not capable of resisting the blast wave will fracture and be further fragmented and moved by the dynamic pressure that immediately follows the shock front. Building contents and people will be displaced and tumbled in the direction of blast wave propagation. In this manner the blast will propagate through the building.

5. NONLINEAR FINITE ELEMENT ANALYSIS PROGRAM

Although explosion experiments are very important in the analysis of blast load effects of structures, computer models and programs have become indispensable in characterizing blast load effects. Simulation of blast load effects on structures is highly nonlinear because of behaviors such as fracture, fragmentation, and flow due to high-pressure sources. In this paper, nonlinear finite element analyses are performed using a program previously developed by the author [15]. This program can be used to predict the nonlinear behavior of any plain, reinforced or prestressed concrete structure that is composed of thin plate members. This includes columns, beams, slabs, shells, girders, shear walls, or any combination of these structural elements. Below is a brief description of material properties and modeling techniques in this program.

5.1 Concrete and reinforcing bar properties

Under the action of rapidly applied loads, the rate of strain increases, which can affect

mechanical properties of structural materials significantly. For blast loading, all material experiments are under monotonic loading and repeated loading is usually not considered. The yielding stress of steel and the compressive strength of concrete are increased by more than 25% which is called high-strain rate effects. Percentage elongation at failure remains approximately unchanged for both concrete and steel. Ultimate strain is slightly reduced, or the strain at maximum stress and rupture remain nearly constant. At last, elastic modulus remain the same for steel, or increase slightly for concrete. Current research shows that strain effects primarily increase structural material strength and have very little influence on the failure strain. Hence, strain rate effect is usually considered a factor of static yield stress. This strain effect factor is only a function of strain rate and material properties. Hence, tensile failure strain can be assumed as 0.002 for concrete cover, 0.005 for concrete core and 0.23 for reinforcing rebar on the basis of static experiments.

The concrete behaves differently under different types and combinations of stress conditions due to the progressive micro-cracking at the interface between the mortar and the aggregates (transition zone). The propagation of these cracks under the applied loads contributes to the nonlinear behavior of the concrete. There are many existing concrete constitutive models to simulate blast load effects. The model accepted for this research is a computational constitutive model for concrete subjected to large strains, high strain rates, and high pressures. The model is similar to smeared crack model, but is expanded to include material damage, strain rate effects, and permanent crushing as a function of the pressure [16]. As shown in Figure 6(a), the uniaxial stress-strain curve of concrete adopted in this study comprises two parts. The ascending branch up to the peak compressive strength is represented by the equation proposed by Ashour and Morley [1]:

$$\sigma = \frac{E_0 \varepsilon}{1 + \left(\frac{E_0}{E_{sc}} - 2\right)\left(\frac{\varepsilon}{\varepsilon_{max}}\right) + \left(\frac{\varepsilon}{\varepsilon_{max}}\right)^2} \tag{1}$$

where E_0 is the initial modulus of elasticity of the concrete, E_{sc} is the secant modulus of the concrete at the peak stress, σ is stress, ε is strain and ε_{max} is the strain at peak stress. The descending, or the strain-softening, branch is idealized by the Bazant *et al.* model [18]:

$$\sigma = \sigma_c \left(\frac{\varepsilon}{\varepsilon_{max}}\right) \exp\left(1 - \varepsilon / \varepsilon_{max}\right) \tag{2}$$

where σ_c is compressive strength of the concrete. For uniaxially loaded concrete, σ_c is equal to f'_c.

For analysis of most plane stress problems, concrete is assumed to behave as a stress-induced orthotropic material. In this study, the orthotropic constitutive relationship developed by Darwin and Pecknold [19] is used for modeling the concrete using the smeared cracking idealization. The constitutive matrix, D, is given by:

$$D = \frac{1}{(1-\nu^2)}\begin{bmatrix} E_1 & \nu\sqrt{E_1E_2} & 0 \\ \nu\sqrt{E_1E_2} & E_2 & 0 \\ 0 & 0 & \frac{1}{4}(E_1+E_2-2\nu\sqrt{E_1E_2}) \end{bmatrix} \tag{3}$$

in which E_1 and E_2 are the tangent moduli in the directions of the material orthotropy, and ν is the Poisson's ratio. The orthotropic material directions coincide with the principal stress directions for the uncracked concrete and these directions are parallel and normal to the cracks for the cracked concrete. The concept of the "equivalent uniaxial strain" developed by Darwin and Pecknold [19] is utilized to relate the increments of stress and strain in the principal directions. Therefore, stress-strain curves similar to the uniaxial stress-strain curves can be used to formulate the required stress-strain curves in each principal direction.

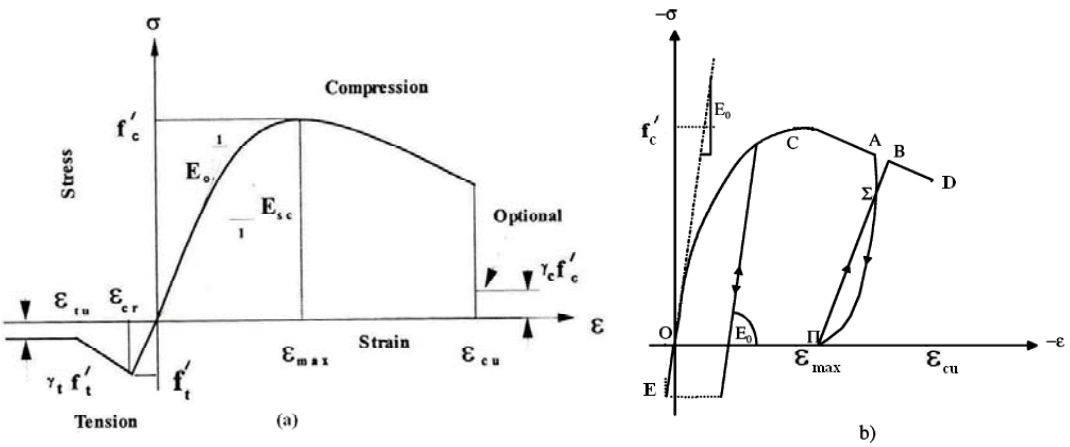

Figure 6. The stress–strain relationship of concrete for (a) monotonic loading; (b) cyclic loading

The strength of concrete, σ_c, and the values of E_1, E_2 and ν are functions of the level of stress, and the stress combinations. The concrete strength when subjected to biaxial stresses is determined using the failure envelope developed by Kupfer *et al.* [20]. The values of E_1 and E_2 for a given stress ratio ($\alpha=\sigma_1/\sigma_2$) are found as the slopes of the σ_1-ε_1 and σ_2-ε_2 curves, respectively. For the descending branches of both compression and tension stress-strain curves, E_i is set equal to a very small number, 0.0001, to avoid computational problems associated with a negative and zero values for E_i. The concrete is considered crushed once the equivalent compressive strain in the principal directions exceeds the ultimate compressive strain of the concrete, ε_{cu}. For determination of the concrete ultimate compressive strain, ε_{cu}, two models for unconfined high and normal-strength concrete (Pastor [21]) and confined concretes (Chung *et al.* [22]) are implemented into the program. In order to eliminate numerical problems after crushing ($\varepsilon>\varepsilon_{cu}$) and cracking of the concrete ($\varepsilon>\varepsilon_{tu}$), a small value is assigned to the compressive and tensile stresses as a fraction of

concrete strength, $\gamma_c f'_c$ and $\gamma_t f'_t$, at a high level of stress (Fig. 6(a)), where parameters γ_c and γ_t define the remaining compressive and tensile strength factors, respectively.

Regarding the stress–strain relationships for cyclic loading, it is important to distinguish between the unloading paths before and after the compression strength (Fig. 6(b)) is exceeded. In the first case, the unloading path is a straight line defined by the elastic modulus E_0 and tensile stresses are still possible. In the second case, the unloading path doesn't reach the tensile region. After exceeding the maximum tensile strength, cracks occur perpendicular to the principal stress direction. Based on a smeared crack model a smeared crack width is then calculated.

5.2 Crack modeling techniques

Cracking of the concrete is one of the important aspects of nonlinear material behaviour of the concrete. Besides reducing the stiffness of the structure, cracks have resulted in redistribution of stresses into the reinforcing steel as well as increasing the bond stress at the steel-concrete interface [23]. Cracking of the concrete is idealized using the fixed smeared cracking model and is assumed to occur when the principal tensile stress at a point (usually a Gauss integration point) exceeds the tensile strength of the concrete. After cracking, the axes of orthotropy are aligned parallel and orthogonal to the crack. The elastic modulus perpendicular to the crack direction is reduced to a very small value, close to zero, and the Poisson effect is ignored. The effect of the crack is smeared within the element by modifying the [D] matrix. If σ_1 exceeds the tensile strength of concrete, f'_t, the material stiffness matrix is defined as (one crack is opened):

$$[D] = \begin{bmatrix} 0 & 0 & 0 \\ 0 & E_2 & 0 \\ 0 & 0 & \beta G \end{bmatrix} \quad \text{where } 0<\beta\leq 1.0 \tag{4}$$

Once one crack is formed, the principal directions are not allowed to rotate, and a second crack can form only when $\sigma_2 > f'_t$, in a direction perpendicular to the first crack. Then,

$$[D] = \begin{bmatrix} 0 & 0 & 0 \\ 0 & 0 & 0 \\ 0 & 0 & \beta G \end{bmatrix} \quad \text{where } 0<\beta\leq 1.0 \tag{5}$$

The shear retention factor, β, with a value of less than unity, serves to eliminate the numerical difficulties that arise if the shear modulus is reduced to zero, and more importantly, it accounts for the fact that cracked concrete can still transfer shear forces through aggregate interlock and dowel action. Due to the bond between the concrete and the steel reinforcement, a redistribution of the tensile stress from the concrete to the reinforcement will occur. In fact, the concrete is able to resist tension between the cracks in the direction normal to the crack; this phenomenon is termed tension-stiffening.

The reinforcing bars are modeled as an elastic strain-hardening material as shown in Figure 7. The reinforcing bars can be modeled either as smeared layers or as individual bars.

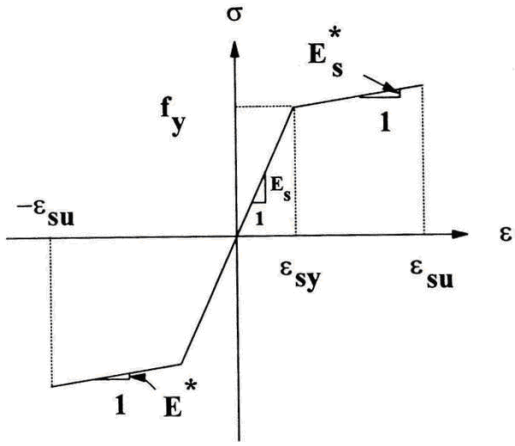

Figure 7. The stress–strain relationship of steel

5.3 Finite element formulation

The element library includes plane membrane and plate bending as well as a facet shell element which is a combination of the plane membrane and plate bending elements. The program employs a layered finite element approach. The structure is idealized as an assemblage of thin constant thickness plate elements with each element subdivided into a number of imaginary layers . Each layer can assume any state – being uncracked, partially cracked, fully cracked, non-yielded, yielded and crushed – depending on the stress or strain conditions. Eight-node brick elements were used to model the concrete. These elements include a smeared crack analogy for cracking in tension zones and a plasticity algorithm to account for the possibility of concrete crushing in compression regions.

5.4 Nonlinear solution

In nonlinear analysis, the total load applied to a finite element model is divided into a series of load increments called load steps. At the completion of each incremental solution, the stiffness matrix of the model is adjusted to reflect nonlinear changes in structural stiffness before proceeding to the next load increment. The Newton–Raphson equilibrium iterations for updating the model's stiffness were used in the nonlinear solutions. Prior to each solution, the Newton–Raphson approach assesses the out-of-balance load vector, which is the difference between the restoring forces and the applied loads. Subsequently, the program carries out a linear solution using the out-of-balance loads and then checks for convergence. If convergence criteria are not satisfied, the out-of-balance load vector is re-evaluated, the stiffness matrix is updated, and a new solution is carried out. This iterative procedure continues until the results converge.

6. VERIFICATION OF ANALYTICAL MODELS

Although experimental tests of RC members provide valuable information about their behavior; these are normally expensive, time-consuming and require considerable human and physical resources. By using nonlinear finite element analysis, it is possible, at comparatively lower cost and effort, to predict the response of RC structures and members.

The capability and accuracy of the finite element program and analytical models in predicting the nonlinear response of RC columns is verified along with a comparison between the analytical and corresponding experimental results.

On February 7, 2003, a 200-kilo car bomb exploded near Club El Nogal in Columbia, killing 25 and wounding 120. Parameters of the column are shown in Table 1. At the start of the test, axial load was applied to the column specimen after that the column was subjected to blast loading. Finite element model of the column is shown in Figure 8. In the finite element model of the column, size of solid element (i.e., mesh size) is taken as 2.5 cm. The column and supports were modeled as volumes. The combined volumes of the concrete and reinforcing bars are shown in Figure 8. Figure 8 illustrates that the rebar shares the same nodes at the points that it intersects with the shear stirrups. The meshing of the reinforcement is a special case compared to the volumes. No meshing of the reinforcement was needed because individual elements were created in the modeling through the nodes created by the mesh of the concrete volume.

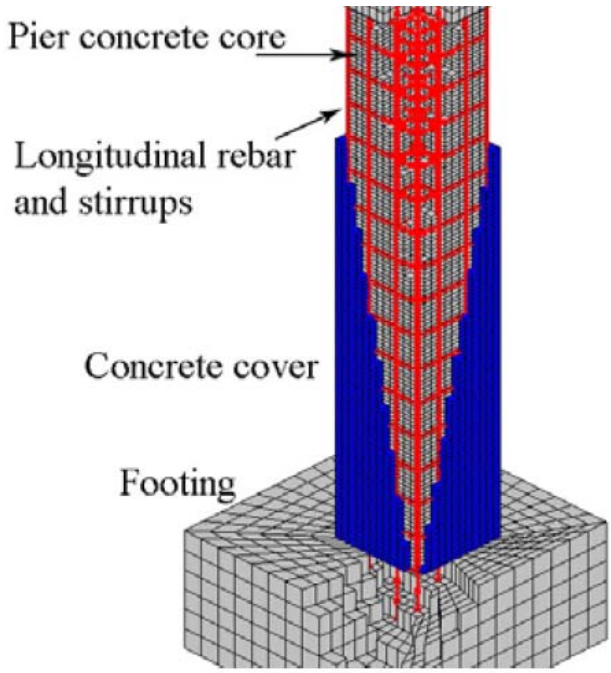

Figure 8. Finite element model of the column

Table 1: Parameters of column in Club El Nogal

Item	Value
Height	3.15 m
Width	90×90 cm
Concrete Strength	21 MPa
Reinforcement Ratio	1.44%

The goal of the comparison between the finite element model and the experimental work is to ensure that the elements, material properties, real constants and convergence criteria are adequate to model the response of the member. Figure 9 shows the simulation of the column subject to blast loads. It is observed from Figure 9 that the concrete cover and a part of concrete core got spelled. The maximum midpoint deflection of the column is approximately 0.35 cm. It is observed that the simulation results match very well with those observed at the blast site. The results indicate that finite element program provide reasonable results and can be used to approximate the nonlinear behavior of RC columns under the blast load.

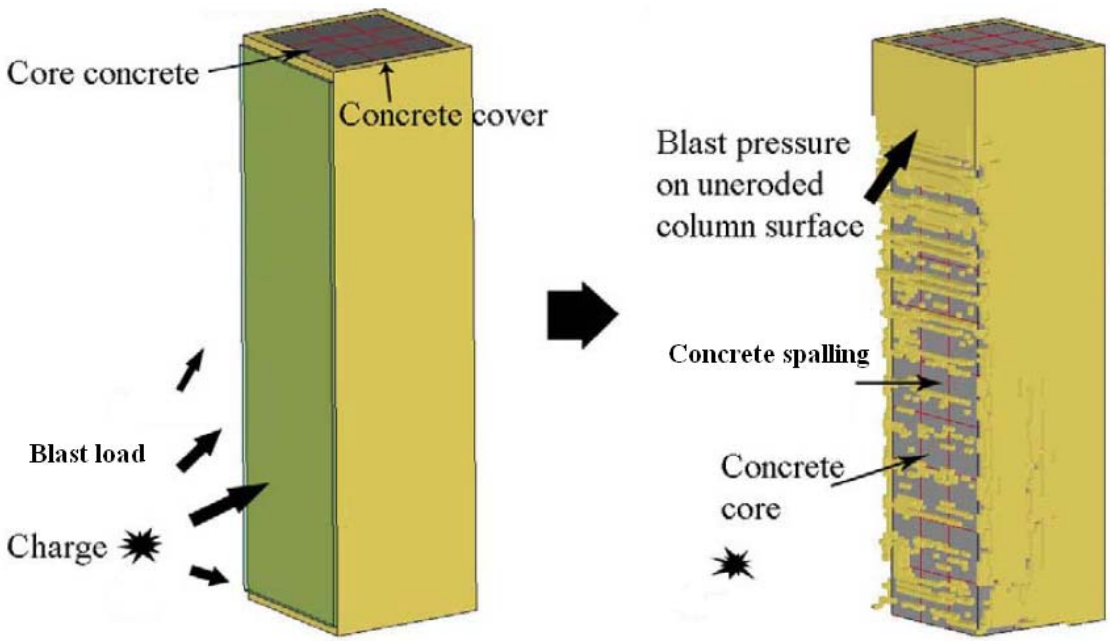

Figure 9. The simulated column before and after loading

7. PARAMETRIC STUDY

In this section, several inelastic analyses have been performed to predict the behavior of RC columns under the blast loading using a nonlinear finite element program. The nonlinear finite element program is capable of predicting large displacement behavior of structures, taking into accounts both geometric nonlinearities and material inelasticity. The fiber modeling approach has been employed to represent the distribution of material nonlinearity along the length and cross-sectional area of the member. Therefore, in this section, the effects of blast loads on three different shapes of RC columns under the blast loading are investigated. Numerical simulations are carried out by developing finite element models for each of columns. Using the simulation results, various failure mechanisms of columns subjected to blast loads are identified.

Most buildings are not specifically designed to resist blast loading. Although they are designed for lateral loads, such as earthquake, they are vulnerable to the large dynamic loading such as blast. Evident have shown that in extreme loading condition, columns near

the blast source can fail severely, leading to progressive building collapse. These columns can be strengthened using steel jacket or composite sheets to enhance the column's shear capacity that prevent building collapse.

Fiber Reinforced Polymer (FRP) materials are composites consisting of high strength fibers embedded in a polymeric resin (Figure 10). Fibers in an FRP composite are the load-carrying elements, while the resin maintains the fibers' alignment and protects them against the environment and possible damage. Among commercially available fibers, those made from carbon exhibit the highest strength and stiffness when compared with steel. The type of fiber is selected based on mechanical properties and durability requirements, while the type of resin depends upon environmental and constructability needs.

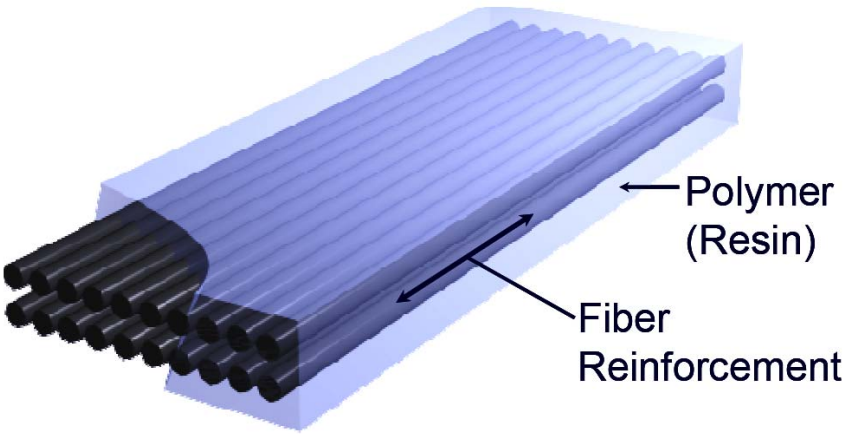

Figure 10. Representation of FRP material

Recent research and development efforts have led to many applications of composite materials for strengthening existing reinforced concrete structures [24]. Ease of construction and broader applications have made fiber composite sheets a more popular choice than plates. While plates are appropriate for flat surfaces and beams, sheets can be used on round (such as columns) and larger (such as walls) surfaces more efficiently and effectively. The primary load-carrying element within a composite is the fiber. Consequently, the fiber has a strong influence on the mechanical characteristics of the composite such as strength and elastic modulus. The resin provides a mechanism for the transfer of load among the fibers. It also protects the fibers from abrasion and other environmental and chemical effects. The fibers can be oriented in a single direction (unidirectional) or several directions, to optimize the performance of the composite. Fiber strengthening technique (by wrapping the element with fiber composite sheets) is a relatively simple process. Fiber strengthening technology is among the most efficient and effective new technologies for seismic retrofitting of RC structures. Its application is quite simple, very non-intrusive to the building's occupants, and not labor intensive – making it one of the more desirable alternatives for the seismic retrofit of existing buildings. The carbon fiber's non-corrosive characteristics and resistance to most chemicals give the carbon fiber strengthening system a considerably longer life than alternative systems. In this section, we address the analysis of RC columns with and

without FRP under the blast loading.

7.1 Square columns

Four blast analyses are done to compare the response of FRP wrapped columns to those of bare (as is) columns. These columns are square with four different widths i.e. 300, 350, 400, 450 mm and are subjected to the same stand-off blast load. Analytical results show that bare RC columns fail severely in shear because of the lack of ductility in its shear behavior and deform in flexure beyond the allowable limit.

All columns are retrofitted with FRP sheets (Figure 11). The FRP sheets have modulus of elasticity of 250 GPa and tensile strengths of 4 GPa. The retrofitted columns are analyzed with the same blast loading. The results show that for the retrofitted columns both shear and moment capacities are improved. The columns remain elastic to some extent and no permanent deformation is apparent. As shown in Figure 12, bare columns yields in shear at the top and bottom. After that, a tensile response in the rebars occurs. The residual column deflection at midheigth is about 300 mm. The time history of the midheight displacement is shown in Figure 13 for both columns i.e. bare and retrofitted columns with the width of 400 mm. FRP retrofitting enable columns to develop their full flextural capability. The peak resistance is about twice that of the unretrofitted column and this increase is maintained until FRP sheet failed.

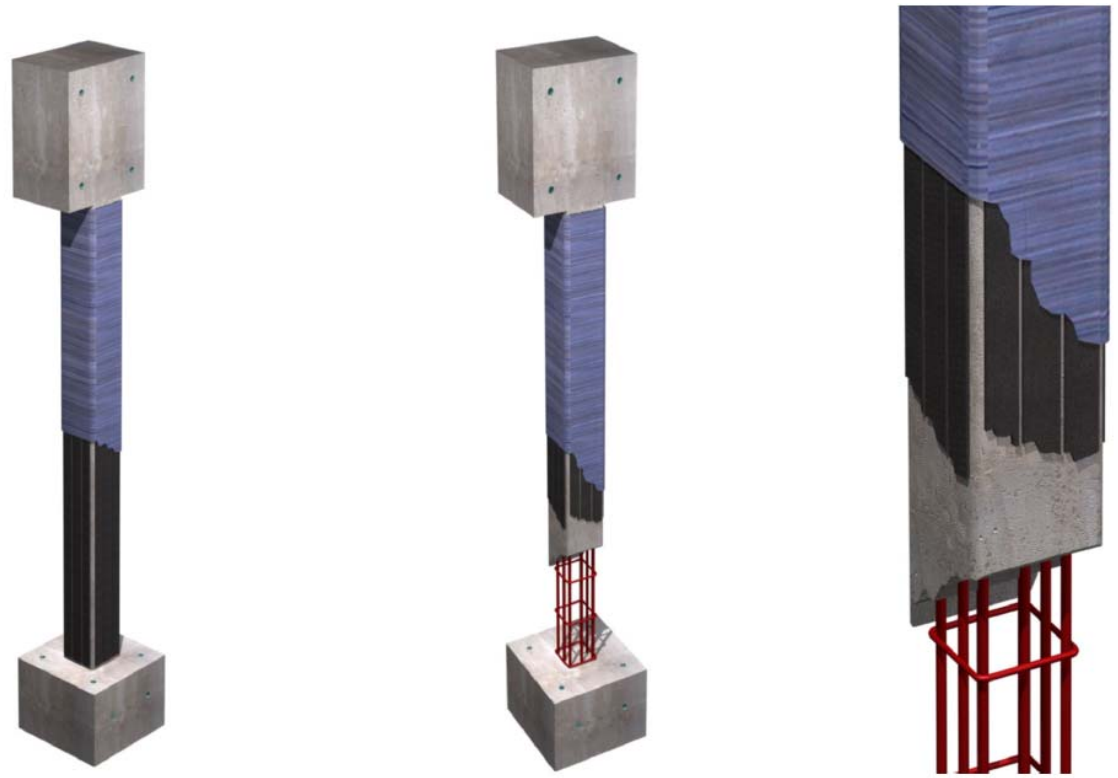

Figure 11. Retrofitting of the square columns with FRP sheets

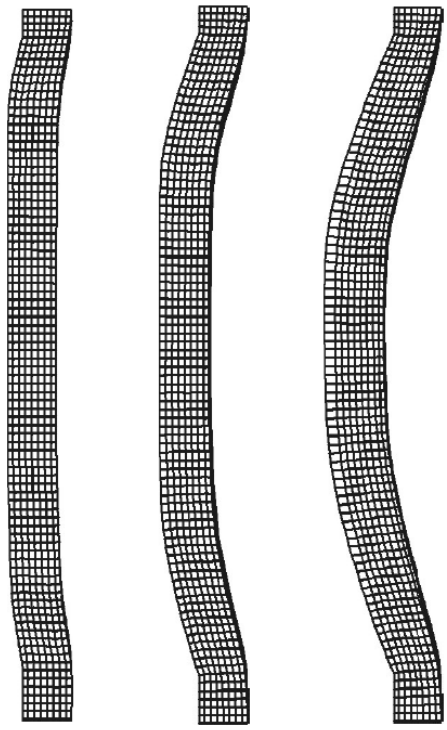

Figure 12. Columns deformed shape under the blast loading

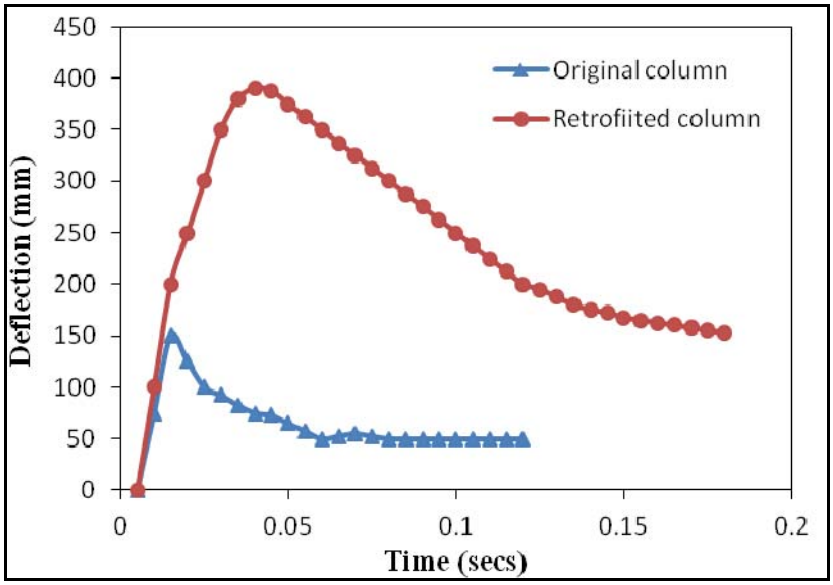

Figure 13. Column predicted mid-height deflection

7.2 Circular column

The blast strengthening of a structure requires the minimization of loss of life by reducing local structural failures. In this section, effect of blast loads on the existing RC circular

columns and its response when retrofitted using FRP is investigated. Different charge weights at variable stand-off distances are considered. Eight-node solid elements with approximate average size of 75 mm are used to model the concrete volume. The finite element mesh of the column section is displayed in Figure 14. The longitudinal reinforcing bars and ties are modeled using 2-node elements. For the modeling of FRP sheets, 4-node shell elements are employed.

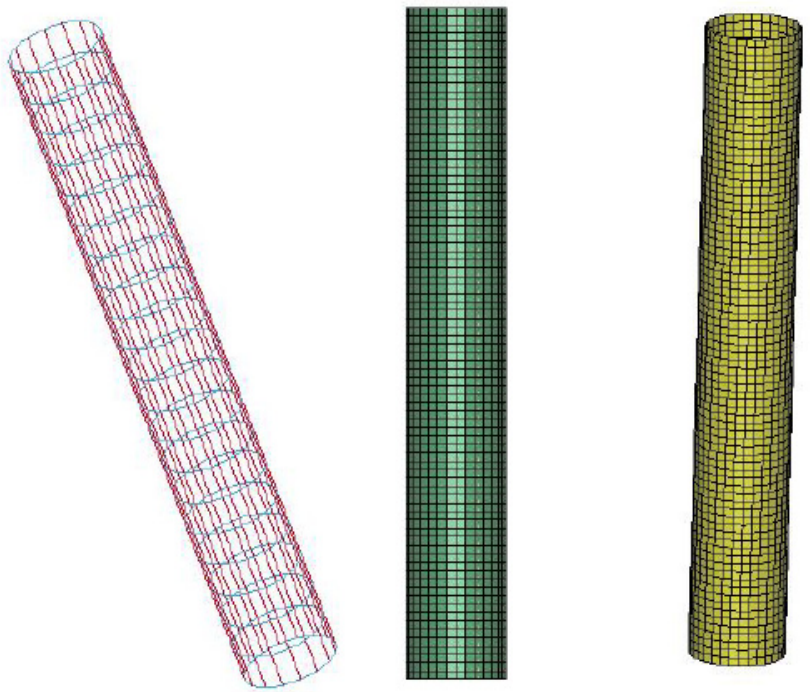

Figure 14. Mesh configuration of circular columns

Perfect bond is assumed between rebar elements and the surrounding concrete volume and also between the FRP and the concrete substrate. Figures 14 also show the mesh of concrete, FRP and reinforcement cage. The charge weights of 150, 300, 500 and 1000 kg at stand-off distances of 1, 3 and 10 m are considered in the study. Both the un-strengthened and FRP-strengthened columns are subjected to these blast loads.

The results show that insignificant damage to the column was not seen and the column (with and without FRP strengthening) are completely destroyed at 1.0 m stand-off distance with 150, 300, 500 and 1000 kg explosive. For bare RC column with charge weight of 300 kg at the stand-off distance of 3 m, concrete was completely destroyed over the bottom third height and in the retrofitted column; damage to concrete was seen at the bottom 0.5 m height of the column. The FRP material had protected the concrete from any severe damage. For RC column with charge weight of 500 kg at the stand-off distance of 10 m, a lateral deflection of 35 mm occurs at the mid-height of bare column and a maximum lateral deflection of 10 mm was yielded in the retrofitted column. Negligible lateral displacement was seen in the column with charge weight of 150 kg at the stand-off distance of 10 m (Figure 15). No damage to concrete core or cover was observed. It is clear that the displacement experienced by the

retrofitted columns is much lower compared with the un-strengthened columns. This demonstrates that FRP strengthening might be a valuable tool in protecting the service integrity of RC columns especially when the blast charge weights are smaller.

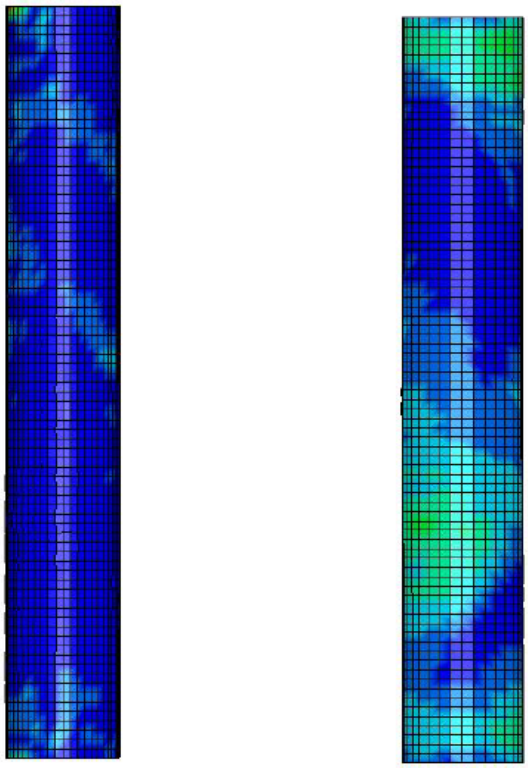

Figure 15. Damage level in bare and retrofitted column for 100 kg charge weight at 10 m stand-off distance

All results showed that composite retrofits can have a beneficial effect on the performance of the columns and therefore prevent progressive collapse. For example, at a stand-off distance of 3 m, with a 150 kg TNT charge, circular column had a 48 mm of lateral displacement. When retrofitted with CFRP composites, the lateral displacement reduced to 18 mm, a 62% decrease. The results show that the retrofitting of column reduces the peak lateral displacement considerably. The retrofitting of column reduces the peak displacement by 21% when the damage to the column is almost negligible, i.e. when the intensity of blast is least severe. A study of all blast cases considered indicates that the reduction of peak displacement varies from 12% for 150 kg charge weight at stand-off distance of 3 m to 76% for 1000 kg charge weight at a stand-off distance of 10 m. Further, there is exponential increase in peak lateral displacement with the reduction in the stand-off distance.

7.3 Rectangular column

A ground floor column (5.4m high) of a multi-storey building is analyzed with two different concrete strength in this case study. The parameter considered is the concrete strength, i.e. 35MPa for normal strength concrete (NSC) column and 70MPa for high strength concrete

(HSC) column. It is found that with increasing concrete compressive strength, the column size can be effectively reduced. In this case the column size was reduced from 450×800 mm for the NSC column down to 350× 700 for the HSC column (Table 2) while the axial load capacities of the two columns are still the same (Figure 16).

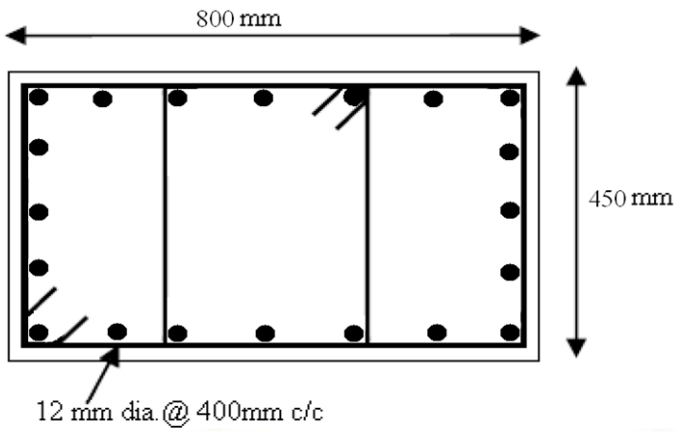

Figure 16. Cross section of rectangular column

Table 2: Concrete grades and member sizes

Column	Sizes	f'_c
NSC	450×800	40
HSC	350×700	80

The simplified triangle shape of the blast load profile is used (Figure 17). The duration of the positive phase of the blast is 2.5 milliseconds. The 3D model of the column (Figure 18) is analyzed using the nonlinear finite element program which takes into account both material nonlinearity and geometric nonlinearity. The strainrate-dependent constitutive model proposed in the previous section is adopted. The effects of the blast loading are modelled in the dynamic analysis to obtain the deflection time history of the column.

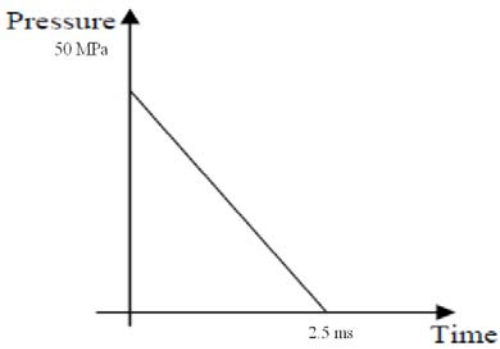

Figure 17. Blast loading

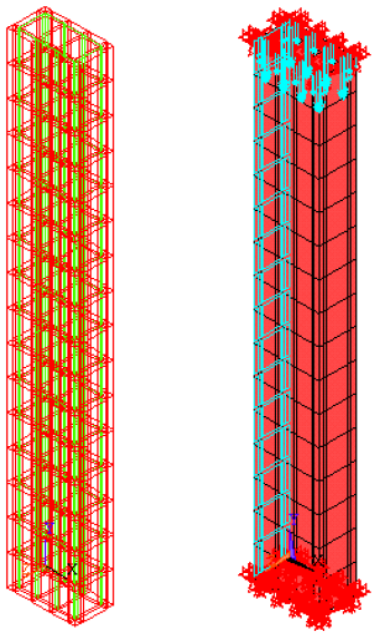

Figure 18. 3D model, mesh configuration and reinforcement of the rectangular column

The stress contour of HSC column is shown in Figure 19. The lateral deflection at mid point and energy flux versus time history of two columns made of NSC and HSC are shown in Figures 20 and 21. The graphs clearly show the lateral resistance of the columns. It can be seen that under this close-range bomb blast both columns failed in shear. However, the 70MPa columns with reduced cross section have a higher lateral deflection, which shows a better energy absorption capacity compared to that of the 35 MPa columns.

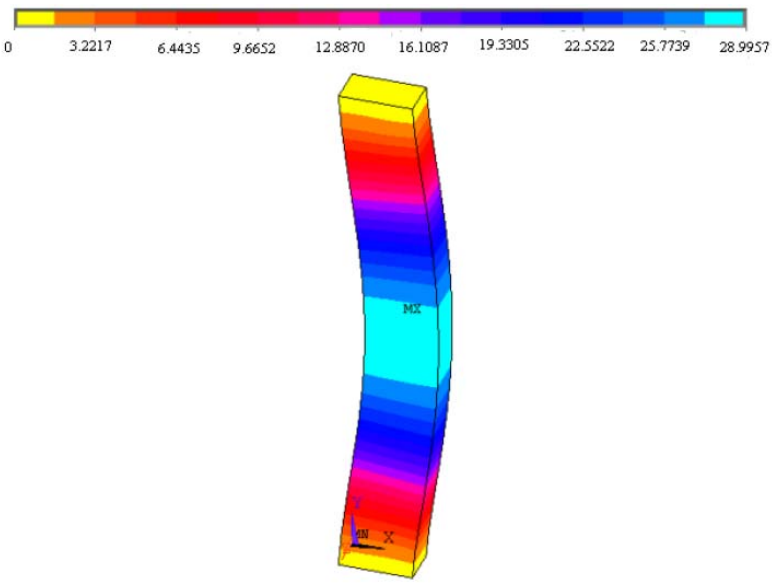

Figure 19. The stress contour of HSC column

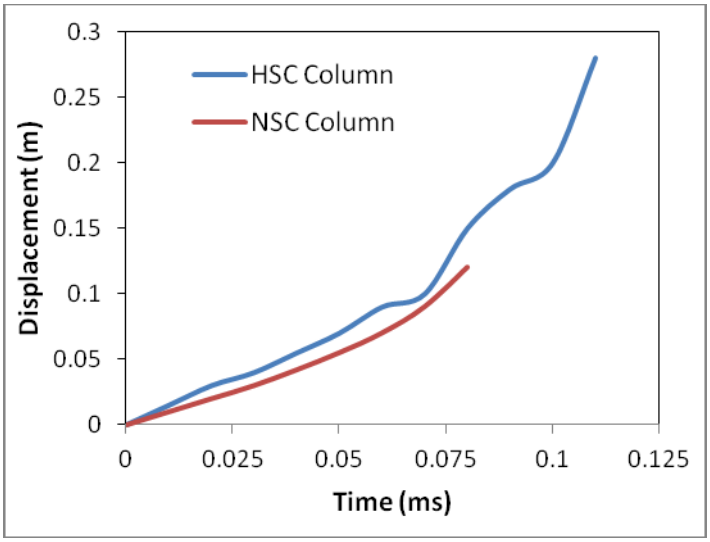

Figure 20. Lateral displacement-time history of rectangular columns

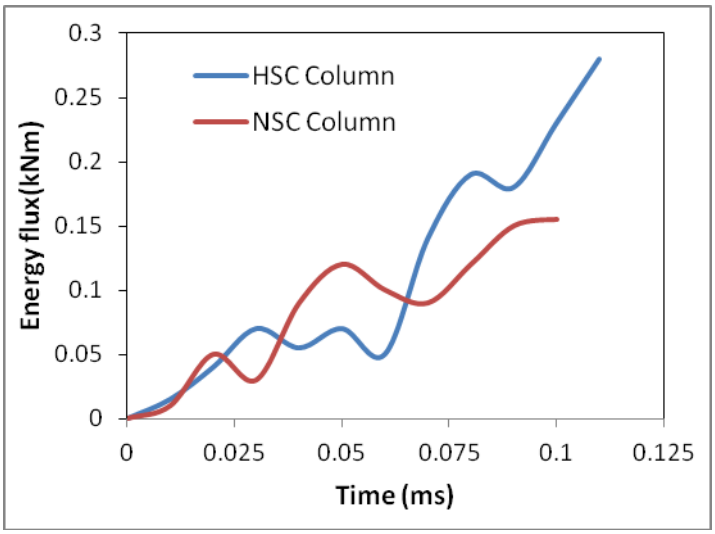

Figure 21. Comparison of energy flux of rectangular columns

The results show that the flexural capacity and the ductility of a reinforced concrete column are significantly increased due to the increase in yield strength of steel and compressive strength of concrete at high strain rate. Therefore, the increase in the material strengths under dynamic conditions may lead to a shift from a ductile flexural failure to a brittle shear failure mode. Also, results of nonlinear finite element analysis of RC frames under blast loading showed that blast loading characterized by pulse-type effects are potentially more damaging in the both ends of elements. These results showed that typical RC buildings can be subjected to large displacement demands at the arrival of the pulse, which require the structure to dissipate considerable input energy in a single cycle. Therefore, as were seen in Figures, all columns need to strengthen with FRP sheets.

7.4 Disscussion

The simulation results showed that the concrete near the bottom section of columns close to blast loads crushed. Strength of column material and rebar detailing in the bottom portion of the column are the key factors affecting this kind of damage. Blast pressure on a column causes the shearing failure at the bottom of a column. Because of high pressure near the top and bottom of RC columns, denser detailing of stirrups may required to prevent occurrence of shear failure.

Concrete surfaces undergo significantly amount of spalling under blast wave loads. During the application of blast loads on concrete surface of a column, some of the blast waves are reflected back from the column surface. This causes a tensile wave effect on the back surface of the column, which causes spalling of concrete. Hence, spalling of concrete is usually more severe on the back surface of a column than on the front surface facing the explosive.

Concrete core of columns is crushed under the impact of high blast loads, resulting in the formation of plastic hinge in columns at locations of high blast loads.

8. CONCLUSION

Iran is a regional power, and holds an important position in international energy security and world economy as a result of its large reserves of petroleum and natural gas. Therefore, it might be exposed at risk. The recognition necessity of risk and the resisting trend is essential for structural engineering.

FRP and polymer retrofitting can significantly increase the blast resistance of a structure by increasing its strength and ductility and reducing fragmentation. The results showed that the stand-off distance plays a very important role in mitigating the adverse effects of a blast. The charge weights of 300 and 500 kg at 3 m stand-off distance may be resisted by the column after retrofitting. However, the increase in the number of layers of FRP may help the column to resist even slightly more intense blasts.

A comparison of the retrofitted RC column with un-retrofitted column cases reveals that even a light retrofitting considered in the study provided considerable resistance to blast loads, and thus contributed greatly to impeding the onset of progressive collapse for moderate blasts. The nature of the failure for FRP-wrapped columns was also less explosive, thereby protecting loss of human life and property. It is evident that increasing the rate of loading will result in increases in strength and stiffness of concrete, yield strength of steel and load-carrying capacity of reinforced concrete flexural members.

Generally, fewer number of damage failure have been observed in a column simulation for a lower level of blast load. With an increase in blast load on a column, number of damage failures is also seen to increase. Columns with higher capacities have a lesser level of damages. Damage mechanisms, such as collapsing of columns, are critical to the service performance of the building and should be prevented through multi-hazard blast resistant design.

REFERENCES

1. Ghayamghamian MR, Hisada Y. Near fault strong motion complexity of the 2003 Bam earthquake (Iran) and low frequency ground motion simulation, *Geophysical Journal International*, **170**(2007) 679-86.
2. Hussein AT. Nonlinear analysis of SDOF system under blast load, *European Journal of Scientific Research*, **45**(2010) 430-7.
3. Luccioni B, Ambrosini D, Danesi R. Blast load assessment using hydrocodes, *Engineering Structures*, **28**(2006) 1736-44.
4. Shi Y, Li ZX, Hao H. A new method for progressive collapse analysis of RC frames under blast loading, *Engineering Structures*, **32**(2010) 1691-703.
5. Khadid A. Blast loaded stiffened plates, *Journal of Engineering and Applied Sciences*, **2**(2007) 456-61.
6. Pandey AK, Kumar R, Paul DK, Trikha DN. Non-linear response of reinforced concrete containment structure under blast loading, *Nuclear Engineering and Design*, **236**(2006) 993-1002.
7. Remennikov AM. A review of methods for predicting bomb blast effects on buildings, *Journal of Battlefield Technology*, **6**(2003) 155-61.
8. Marchand KA, Alfawakhiri F. Blast and progressive collapse, *Fact for Steel Buildings*, AISC report, USA, 2005.
9. Dharaneepathy MV, Rao MNK, Santhakumar AR. Critical distance for blast resistance design, *Computers and Structures*, 54 (1995) 587-595.
10. Shope RL. Response of wide flange steel columns subjected to constant axial load and lateral blast load, Civil Engineering Department, Blacksburg, Virginia, 2006.
11. Borvik T, Hanssen AG, Langseth M, Olovsson L. Response of structures to planar blast loads – A finite element engineering approach, *Computers and Structures*, **87**(2009) 507-20.
12. Ngo T, Mendis P, Gupta A, Ramsay J. Blast loading and blast effects on structure, The University of Melbourne, Australia, 2007.
13. Starossek U. Progressive collapse of bridges - Aspects of analysis and design. *International Symposium on Sea-Crossing Long-Span Bridges*, Mokpo, Korea, 2006. CD – ROM.
14. Bazant ZP, Verdure M. Mechanics of progressive collapse: Learning from World Trade Center and building demolitions. *Journal of Engineering Mechanics*, **133**(2007) 308-19.
15. Mortezaei A. A program for three-dimensional nonlinear dynamic analysis of reinforced concrete buildings, School of Civil Engineering, The University of Queensland, Brisbane, Queensland, 2009.
16. Holmquist TJ, Johnson GR, Cook WH. A computational constitutive model for concrete subjected to large strains, high strain rates, and high pressures. *Proceedings 14th International Symposium on Ballistics*, Quebec, Canada, 1993, pp. 591-600.
17. Ashour AF, Morley CT. Three-dimensional nonlinear finite element modeling of reinforced concrete structures, *Finite Elements in Analysis and Design*, **15**(1993) 43-55.
18. Bazant ZP, Belytschko T, Yul-Woong H, Ta-Peng C. Strain-softening materials and finite-element solutions, *Computers & Structures*, **23**(1986) 163-80.
19. Darwin D, Pecknold DA. Nonlinear biaxial stress-strain law for concrete, *ASCE*

Journal of the Engineering Mechanics Division, **103**(1977) 229-41.
20. Kupfer HB, Gerstle KH, Rusch H. Behavior of concrete under biaxial stresses, *ACI Structural Journal*, **66**(1969) 656-66.
21. Pastor JA. *High-strength concrete beams*, Ph.D. Thesis, Cornell University, New York, Ithaca, 1986.
22. Chung H, Yang K, Lee Y, Eun H. Stress–strain curve of laterally confined concrete, *Engineering Structures*, **24**(2002) 1153-63.
23. Sundara Raja Iyengar KT, Raviraj S, Jayaram TN. Analysis of crack propagation in strain-softening beams, *Engineering Fracture Mechanics*, **69**(2002) 761-78.
24. Mortezaei A, Ronagh HR, Kheyroddin A. Seismic evaluation of FRP strengthened RC buildings subjected to near-fault ground motions having fling step. *Composite Structures*, **92**(2010) 1200-11.